

# INNOVIZATION: Innovative Design Principles Through Optimization

Kalyanmoy Deb and Aravind Srinivasan  
Kanpur Genetic Algorithms Laboratory (KanGAL)  
Indian Institute of Technology Kanpur  
Kanpur, PIN 208016, India  
Email: {deb,aravinds}@iitk.ac.in  
<http://www.iitk.ac.in/kangal/pub.htm>

**KanGAL Report Number 2005007**

## Abstract

This paper introduces a new design methodology (we called it an “innovization” task) in the context of finding new and innovative design principles by means of optimization techniques. Although optimization algorithms are routinely used to find an optimal solution corresponding to an optimization problem, the task of innovization stretches the scope beyond an optimization task and attempts to unveil new and innovative design principles relating to decision variables and objectives, so that a deeper understanding of the problem can be obtained. After describing the innovization procedure and its difference from a standard optimization procedure, the innovization procedure is applied to a number of engineering design problems. The variety of problems chosen in the paper and the resulting innovations obtained for each problem amply demonstrate the usefulness of the innovization task. The results should encourage a wide spread applicability of the proposed innovization procedure (which is not simply an optimization procedure) to other problem-solving tasks.

**Keywords:** Innovative design, optimization, engineering design, evolutionary optimization, multi-objective optimization, commonality principles, Pareto-optimal solutions.

## 1 Introduction

Innovation, defined in Oxford American Dictionary as ‘the act of introducing a new process or the way of doing new things’ has always fascinated man. In the context of engineering design of a system, a product or a process, researchers and applicationists constantly look for innovative solutions. Unfortunately, there exist very few scientific and systematic procedures for achieving such innovations. Goldberg [12] narrates that a competent genetic algorithm – a search and optimization procedure based on natural evolution and natural genetics – can be an effective mean to arrive at an innovative design for a single objective scenario.

In this paper, we extend Goldberg’s argument and describe a systematic procedure involving a multi-objective optimization task and a subsequent analysis of optimal solutions to arrive at a deeper understanding of the problem, and not simply to find a single optimal (or innovative) solution. In the process of understanding insights about the problem, the systematic procedure suggested here may often decipher new and innovative design principles which are common to optimal trade-off solutions and were not known earlier. Such commonality principles among multiple solutions should provide a reliable procedure of arriving at a ‘blue-print’ or a ‘recipe’ for solving the problem in an optimal manner. Through a number of engineering design problems,

we describe the proposed ‘innovization’ process and present resulting *innovized* design principles which are useful, not obvious from the appearance of the problem, and also not possible to achieve by a single-objective optimization task.

In the remainder of the paper, we describe the importance of considering multiple conflicting objectives in an innovative design task in Section 2. Thereafter, we present the proposed innovization procedure in Section 3. The innovization task is illustrated by applying the procedure on a number of engineering design problems in Sections 4 to 8. Finally, conclusions are made in Section 9.

## 2 Multiple Conflicting Objectives of Design

The main crux of the proposed innovization procedure involves optimization of at least two *conflicting* objectives of a design. When a design is to be achieved for a single goal of minimizing *size* of a product or of maximizing *output* from the product, usually one optimal solution is the target. When optimized, the optimal solution portrays the design, fixes the dimensions, and implies not much more. Although a sensitivity analysis can provide some information about the relative importance of constraints, they only provide local information close to the single optimum solution. Truly speaking, such an optimization task of finding a single optimum design does not often give a designer any deeper understanding than what and how the optimum solution should look like. After all, how much a single (albeit optimal) solution in the entire search space of solutions can offer to anyone?

Let us now think of an optimum design procedure in the context of two or more conflicting goals. Say, we are interested in the design of a product for minimum size and for maximum output simultaneously. Ideally, such a bi-objective optimization task results in a set of optimal solutions, known as Pareto-optimal solutions, each portraying a trade-off between the two objectives [19, 6]. Out of these optimal solutions lies a solution (say solution A) which is the best for size consideration and a hopefully a different solution (say solution B) which is the best for output consideration. There also lie a host of many other solutions which are not as good as A in terms of size or not as good as B in terms of delivered output, but these intermediate solutions are good compromises to solutions A and B. There exist a plethora of classical and evolutionary approaches to arrive at a number of such Pareto-optimal solutions iteratively and reliably [6, 3, 2, 19]. However, we are not simply interested in finding a set of such optimal trade-off solutions, rather find them and analyze them for discovering some interesting commonality principles in them.

In the design of minimizing size of a product, it is intuitive that the obtained optimal design will correspond to having as small a dimension as possible. Visibly, such a minimum-sized solution will look small and importantly will often not be able to deliver too much of an output. If we talk about the design of an electric induction motor involving armature radius, wire diameter and number of wiring turns as design variables and the design goal is to minimize the size of the motor, possibly we shall arrive at a motor which will look small and will deliver only a few horsepower (as shown as solution A in Figure 1), just enough to run a pump for lifting water to a two-storey building. On the other hand, if we design the motor for the maximum delivered power using the same technology of motoring, we would arrive at a motor which can deliver, say, a few hundreds of horsepower, needed to run a compressor in an industrial air-conditioning unit (solution B in Figure 1). However, the size and weight of such a motor will be substantially large. If we let use a bi-objective optimization method of minimizing size and maximizing delivered power simultaneously, we shall arrive at these two extreme solutions and a number of other intermediate solutions (as shown in the figure) with different trade-offs in size and power, including motors which can be used in an overhead crane to hoist and maneuver a load, motors delivering 50 to

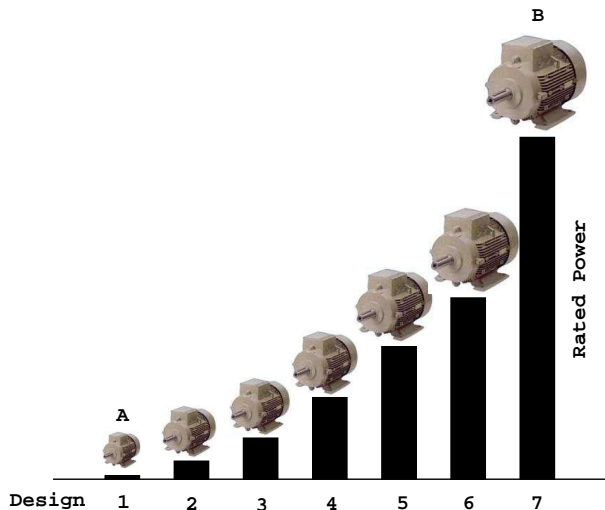


Figure 1: Trade-off designs show a clear conflict between motor size and power delivered in a range of TEFC three-phase squirrel cage induction motors (data taken from Siemens Ltd. [17]). Despite the differences, are there any similarities in their designs?

70 horsepower which can be used to run a machining center in a factory, and motors delivering about a couple of hundred horsepower which can be used as an industrial exhaust fan.

If we now line up all such motors according to the worse order of one of the objectives, say their increased size, in the presence of two conflicting objectives, they would also get sorted in the other objective in an opposite sense (in their increased output). Obtaining such a wide variety of solutions in a single computational effort is itself a significant matter, discussed and demonstrated in various evolutionary multi-objective optimization (EMO) studies in the recent past [6, 3]. Here, we suggest a post-optimality analysis which should result in a set of innovized principles about the design problem, which we describe next.

After the multi-objective optimization task, we have a set of optimal solutions specifying the design variables and their objective trade-offs. We can now analyze these solutions to investigate if there exist some *common* principles among all or many of these optimal solutions. In the context of the motor design task, it would be interesting to see if all the optimal solutions have an identical wire diameter or have an armature diameter proportional or in some relation to the delivered power! If such a relationship among design variables and objective values exist, it is needless to say that they would be of great importance to a designer. Such information will provide a plethora of knowledge (or recipe) of how to design the motor in an optimal manner. With such a recipe, the designer can later design a new motor for a new application without resorting to solving a completely new optimization problem again. Moreover, the crucial relationship among design variables and objectives will also provide vital information about the theory of design of a motor which can bring out limitations and scopes of the existing procedure and spur new and innovative ideas of designing an electric motor.

Such a task has a third dimension in the context of practices in industries. Successful industries standardize their products for reuse, easier maintenance and also for cost reduction. For industries interested in producing a range of products (such as electric motor manufacturing companies produce motors of a particular type ranging from a few horsepower to a few hundreds of horsepower), if some commonality principles of their designs can be found, this may help save inventory costs by keeping only a few common types of ingredients and raw materials (such as wires, armatures etc.) and also may help simplify the manufacturing process, in addition to

cutting down the need for specialized man-powers.

It is argued elsewhere [7] that since the Pareto-optimal solutions are not any arbitrary solutions, rather solutions which mathematically must satisfy the so-called Fritz-John necessary conditions (involving gradients of objective and constraint functions) [13], in engineering and scientific systems and problems, we may be reasonably confident in claiming that there would exist some commonalities (or *similarities*) among the Pareto-optimal solutions which will ensure their optimality. On the other hand, there would exist some *dissimilarities* among them which will make them different from each other and place them on various locations on the Pareto-optimal frontier providing an optimal trade-off among objectives. Whether such similarities exist for all solutions on the Pareto-optimal front or some kind of similarity exist partially among solutions on a part of the Pareto-optimal front and another kind of similarity exists in another part of the front or there exist hierarchical (or level-wise) similarities (some kind to all and some sub-kind to a portion of the front) are matters which may vary from problem to problem. Whatever is the extent of commonalities, if exist, must portray some design principles which are worth knowing. We argue and demonstrate amply in the subsequent sections that such design principles deciphered from the obtained Pareto-optimal solutions may often bring out new and innovative principles which were unknown earlier. They are also useful in design activities and provide a better understanding of parameter interactions. Since these innovative principles are derived through the outcome of a carefully performed optimization task, we call this procedure an act of ‘innovization’ – a process of obtaining innovative solutions and design principles through optimization.

### 3 Innovization Procedure

As described above, the analysis of the optimized solutions will result in worthwhile design principles, if the trade-off solutions are really close to the optimal solutions or if they are exactly on the Pareto-optimal frontier. Since for engineering and complex scientific problem-solving, we need to use a numerical optimization procedure and since in such problems, the exact optimum is not known a priori, adequate experimentation and verification must have to be done first to gain confidence about the closeness of the obtained solutions to the actual Pareto-optimal front. In all case studies performed here, we have used the well-known elitist non-dominated sorting genetic algorithm or NSGA-II [8] as the multi-objective optimization tool. NSGA-II begins its search with a random population of solutions and iteratively progresses towards the Pareto-optimal front so that at the end of a simulation run, multiple trade-off optimal solutions are obtained simultaneously. Due to its simplicity and efficacy, NSGA-II is adopted in a number of commercial optimization softwares and has been extensively applied to various multi-objective optimization problems in the past few years. For a detail procedure of NSGA-II, readers are referred to the original study [8]. The NSGA-II solutions are then clustered to identify a few well-distributed solutions. The clustered NSGA-II solutions are then modified by using a local search procedure (we have used Benson’s method [1, 6] here). The obtained NSGA-II-cum-local-search solutions are then verified by two independent procedures:

1. The extreme Pareto-optimal solutions are verified by running a single-objective optimization procedure (a genetic algorithm is used here) independently on each objective function subjected to satisfying given constraints.
2. Some intermediate Pareto-optimal solutions are verified by using the normal constraint method (NCM) [18] starting at different locations on the hyper-plane constructed using the individual best solutions obtained from the previous step.

When the attainment of optimized solutions and their verifications are made, ideally a data-mining strategy must be used to automatically evolve design principles from the combined data of

optimized design variables and corresponding objective values. By no means this is an easy task and is far from being a simple regression task of fitting a model over a set of multi-dimensional data. We mentioned some such difficulties earlier: (i) there may exist multiple relationships which are all needed to be found by the automated programming, thereby requiring to find multiple solutions to the problem simultaneously, (ii) a relationship may exist partially to the data set, thereby requiring a clustering procedure to identify which design principles are valid on which clusters, and (iii) since optimized data may not exactly be the optimum data, exact relationships may not be possible to achieve, thereby requiring to use fuzzy rule or rough set based approaches. While we are currently pursuing various data-mining and machine learning techniques for an automated learning and deciphering of such important design principles from optimized data set, in this paper we mainly use visual and statistical comparisons and graph plotting softwares for the task.

We present the proposed innovization procedure here:

**Step 1:** Find individual optimum solution for each of the objectives by using a single-objective GA (or sometimes using NSGA-II by specifying only one objective) or by a classical method. Thereafter, note down the *ideal* point.

**Step 2:** Find the optimized multi-objective front by NSGA-II. Also, obtain and note the *nadir* point<sup>1</sup> from the front.

**Step 3:** Normalize all objectives using ideal and nadir points and cluster a few solutions  $Z^{(k)}$  ( $k = 1, 2, \dots, 10$ ), preferably in the area of interest to the designer or uniformly along the obtained front.

**Step 4:** Apply a local search (Benson’s method [1] is used here) and obtain the modified optimized front.

**Step 5:** Perform the normal constraint method (NCM) [18] starting at a few locations to verify the obtained optimized front. These solutions constitute a reasonably confident optimized front.

**Step 6:** Analyze the solutions for any commonality principles as plausible innovized relationships.

Since the above innovization procedure is expected to be applied to a problem once and for all, designers may not be quite interested in the computational time needed to complete the task. However, if needed, the above procedure can be made faster by parallelizing Steps 1, 2, 4 and 5 on a distributed computing machine.

We now illustrate the working of the above innovization procedure on a number of engineering applications. In all problems solved in this paper, we use sufficiently large population size and run an evolutionary multi-objective optimization algorithm (NSGA-II) for sufficient generations so as to have confidence on the obtained trade-off frontier.

## 4 Two-Member Truss Design

We begin with a three-variable, two-objective truss design problem. This problem was originally studied using the  $\epsilon$ -constraint method [2, 19] and later by an evolutionary approach [6], but was never attempted to verify the optimality of the obtained solutions. The truss (Figure 2) has to carry a certain load without elastic failure. We consider two objectives of design: (i) minimize

---

<sup>1</sup>It is interesting to note that finding a set of trade-off Pareto-optimal solutions using an evolutionary multi-objective optimization (EMO) procedure is one way of arriving at the nadir point. Finding the nadir point is an important task in the classical multi-criterion decision-making approaches and is also reported to be a difficult task [15].

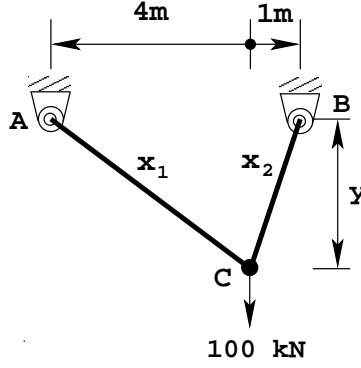


Figure 2: A two-membered truss structure.

total volume of truss members and (ii) minimize the maximum stress developed in both members (AC and BC) due to the application of the 100 kN load. There are three decision variables: cross-sectional area AC ( $x_1$ ) and BC ( $x_2$ ) measured in  $\text{m}^2$  and the vertical distance between A (or B) and C ( $y$ ) measured in m. The non-linear optimization problem is given as follows:

$$\begin{aligned}
 &\text{Minimize } f_1(\vec{x}, y) = x_1\sqrt{16 + y^2} + x_2\sqrt{1 + y^2}, \\
 &\text{Minimize } f_2(\vec{x}, y) = \max(\sigma_{AC}, \sigma_{BC}), \\
 &\text{Subject to } \max(\sigma_{AC}, \sigma_{BC}) \leq S_{\max}, \\
 &\quad 0 \leq x_1, x_2 \leq A_{\max}, \\
 &\quad 1 \leq y \leq 3.
 \end{aligned} \tag{1}$$

Using the dimensions and loading specified in Figure 2, it can be observed that member AC is subjected to  $20\sqrt{16 + y^2}/y$  kN load and member BC is subjected to  $80\sqrt{1 + y^2}/y$  kN load. The stresses are calculated as follows:

$$\sigma_{AC} = \frac{20\sqrt{16 + y^2}}{yx_1}, \tag{2}$$

$$\sigma_{BC} = \frac{80\sqrt{1 + y^2}}{yx_2}. \tag{3}$$

Here, we limit the stresses to  $S_{\max} = 1(10^5)$  kPa and cross-sectional areas to  $A_{\max} = 0.01$   $\text{m}^2$ . All three variables are treated as real-valued and the simulated binary crossover (SBX) with  $\eta_c = 10$  and the polynomial mutation operator with  $\eta_m = 50$  are used [6]. All constraints are handled using the constraint-tournament approach developed elsewhere [6]. Figure 3 shows all non-dominated solutions obtained by NSGA-II. Although the trade-off between the two objectives is clear from the figure, we perform two other studies to gain confidence about optimality of these solutions. First, we employ a single-objective genetic algorithm to find the optimum of individual objective functions subjected to the constraint and variable bounds. Figure 3 marks these two solutions as '1-obj' solutions. It is evident that NSGA-II front extends to these two extreme solutions. Next, we use the NCM method [18] with different starting points from a line joining the two extreme solutions. The solution found at the end of each optimization is shown in the figure as well. Since these solutions fall on the NSGA-II front, it gives us confidence that the obtained NSGA-II non-dominated solutions are close to the Pareto-optimal front (if not on the front).

#### 4.1 Innovized Principles

Before we discuss the NSGA-II solutions, we perform an exact analysis to find the Pareto-optimal solutions. The problem, although simple mathematically, is a typical optimization problem having

two resource terms in objectives involving variables  $x_1$  and  $x_2$  each and interlinking them with another variable  $y$ . For such problems, the optimum occurs when the identical resource allocation between two terms in both objective and constraint functions are made:

$$x_1\sqrt{16+y^2} = x_2\sqrt{1+y^2}, \quad (4)$$

$$\frac{20\sqrt{16+y^2}}{yx_1} = \frac{80\sqrt{1+y^2}}{yx_2}. \quad (5)$$

Thus, every optimum solution is expected to satisfy both the above equations, yielding  $y = 2$  and  $x_1/x_2 = 0.5$ . Using  $y = 2$  m in the expression for the first (volume) objective, we can also obtain  $x_2 = V/2\sqrt{5}$  m<sup>2</sup>, where  $V$  is the volume (in m<sup>3</sup>) of the structure. Substituting these values to the objective functions  $V = f_1$  and  $S = f_2$ , we also obtain  $SV = 400$  kN – an inverse relationship between the objectives. Thus, the solutions in the Pareto-optimal front are given in terms of volume  $V$ , as follows:

$$x_1 = \frac{V}{4\sqrt{5}} \text{ m}^2, \quad x_2 = \frac{V}{2\sqrt{5}} \text{ m}^2, \quad y = 2 \text{ m}, \quad S = 400/V \text{ kPa}.$$

When the variable  $x_2$  reaches its maximum limit, that is, at the transition point,  $V = 0.04472$  m<sup>3</sup> and  $S = 8,944.26$  kPa, and  $x_2$  cannot be increased any further. Interestingly, volume  $V$  can still be increased in an optimal manner, as we shall see later.

The inset plot (drawn with a logarithmic scale of both axes) in Figure 3 shows this interesting aspect of the obtained front. There are two distinct behaviors of the optimal front around the transition point T marked in the figure: (i) one spanning from the smallest-volume solution to about a volume of about 0.04478 m<sup>3</sup> (point T), and (ii) another spanning from this transition point till the smallest-stress solution. The extreme solutions and this intermediate solution, obtained

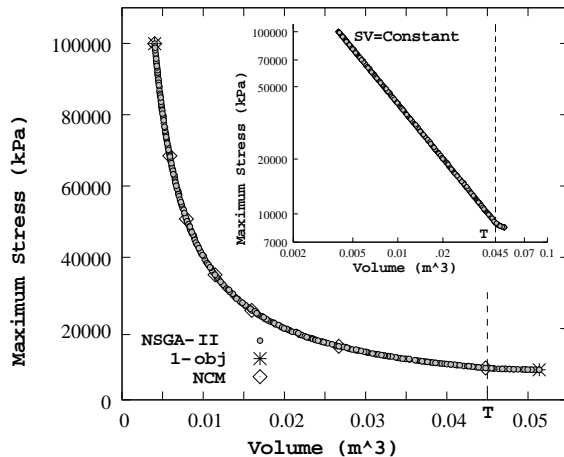


Figure 3: NSGA-II solutions obtained for the two-member truss structure problem.

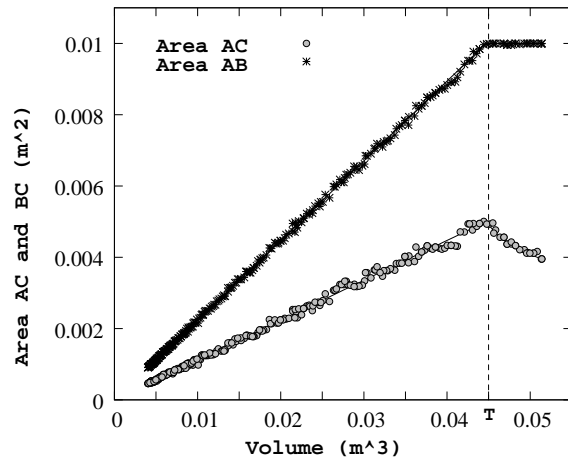


Figure 4: Variation of  $x_1$  and  $x_2$  for the truss structure problem.

by NSGA-II, are tabulated in Table 1. An investigation on the values of the decision variables reveals the following innovations:

1. The inset plot in Figure 3 reveals that for optimal structures, maximum stress ( $S$ ) developed is inversely proportional to the volume ( $V$ ) of the structure, that is,  $SV = \text{constant}$ , as was predicted above. When a straight line is fitted with the logarithm of two objective values,  $SV = 402.2$  relationship is found.

Table 1: Two extreme solutions and an interesting intermediate solution (T) for the two-member truss design problem are presented.

Solution	$x_1$ (m <sup>2</sup> )	$x_2$ (m <sup>2</sup> )	$y$ (m)	$f_1$ (m <sup>3</sup> )	$f_2$ (kPa)
Min. Volume	4.60(10 <sup>-4</sup> )	9.05(10 <sup>-4</sup> )	1.935	0.004013	99,937.031
Intermediate (T)	49.30(10 <sup>-4</sup> )	99.89(10 <sup>-4</sup> )	2.035	0.044779	8,945.610
Min. of max. stress	39.54(10 <sup>-4</sup> )	100.00(10 <sup>-4</sup> )	3.000	0.051391	8,432.740

- The inset plot also reveals that the transition occurs at  $V = 0.044779$  m<sup>3</sup>, close to the theoretical value.
- To achieve a solution with smaller maximum stress (and larger volume) optimally, both cross-sectional areas (AC and BC) need to be increased linearly with volume, as shown in Figure 4. The figure also plots the mathematical relationships ( $x_1$  and  $x_2$  versus  $V$ ) obtained earlier with solid lines, which can be barely seen as the obtained NSGA-II solutions fall on top of these lines.
- A further investigation reveals that the ratio between these two cross-sectional areas is almost 1:2 and the vertical distance ( $y$ ) takes a value close to 2 m for all solutions.
- Figure 5 reveals that the stresses developed on both members (AC and BC) are identical for any optimized solution.

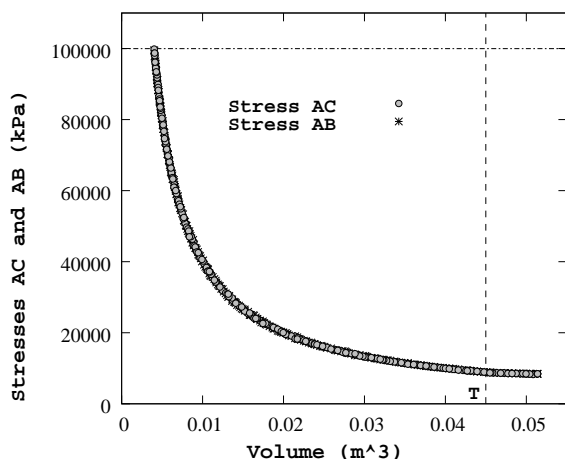


Figure 5: Variation of stresses in AC and BC of the two-member truss structure problem.

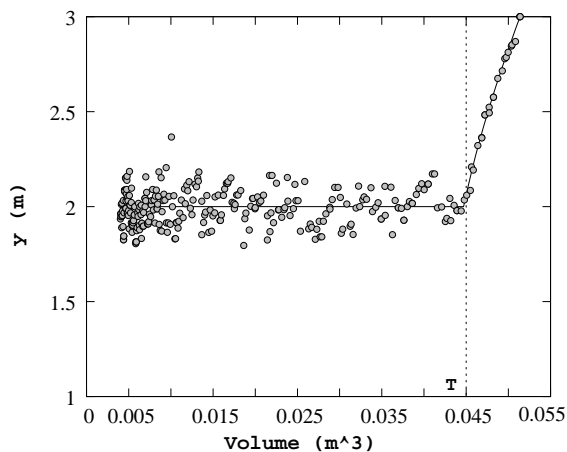


Figure 6: Variation of  $y$  for the two-member truss structure problem.

These are interesting properties about the design problem which may not be so intuitive to a designer. But, the above innovized principles can be explained from the mathematical formulation described above. Thus, although these optimality conditions can be derived mathematically from the problem formulation given in Equation 1 in this simple two-membered truss-structure design problem, they may be often tedious and difficult to achieve exactly for large-sized and complex problems. Applying a numerical optimization technique and investigating the optimized solutions have the potential of revealing such important innovative principles of design.

For solutions beyond the intermediate solution (T), a different scenario occurs. Since  $x_2$  reaches its upper limit (0.01m chosen here) at this critical point,  $x_2$  cannot be increased further

and it remains fixed to this upper limit for all larger volume solutions. However, two optimality properties – (i) the stresses in both members continue to have identical values and (ii) relationship between two cross-sectional sizes dictated by Equation 4 continues to hold good. But, now  $x_1$  and  $y$  gets adjusted in a different manner:  $y$  (in m) is increased and  $x_1$  (in m<sup>2</sup>) is reduced with an increase in overall volume ( $V$  in m<sup>3</sup>) of the structure, as given below:

$$y = \sqrt{3200V^2 + 40V\sqrt{6400V^2 - 12}} - 4, \quad (6)$$

$$x_1 = 0.0025\sqrt{\frac{16 + y^2}{1 + y^2}}. \quad (7)$$

Beyond this critical point (T), since  $x_2$  cannot be increased any further, the only way to reduce the stresses is to increase  $y$  in a manner so as to make the stresses in both members equal. An increase of  $y$  increases the length of the members, but decreases the component of the applied load on each member. Thus, a smaller cross-sectional area can be used to withstand the smaller load causing a smaller developed stress. Equation 7 shows how the cross-section must be decreased as a function of  $y$ .

Following observations can be made from the obtained solutions:

1. All NSGA-II solutions having a volume larger than the transition solution (T) is found to have a fixed  $x_2 = 0.01$  m<sup>2</sup> (upper limit of  $x_2$ ).
2. Figure 4 also verifies that beyond the transition point T,  $x_1$  decreases with volume.
3. To verify the variation of  $y$  with  $V$  given in Equation 6, Figure 6 is plotted with NSGA-II solutions and with Equation 6. The optimal relationship between the two objectives is as follows:  $SV = (4 + y^2)/(0.01y)$ . Since for Pareto-optimal solutions having  $V > 0.04472$  m<sup>3</sup>, the parameter  $y$  increases with  $V$ , the quantity  $SV$  increases with  $V$ , as depicted in the inset plot of Figure 3.

Some of the above properties (such as, the existence and location of the transition point, cross-sectional area  $x_2$  being constant beyond the transition point, and reduction of  $x_1$  beyond the transition point to increase  $V$  optimally) are difficult to comprehend from the problem formulation and importantly are also difficult to obtain by any other means, including multiple single-objective optimizations of different weighted-sum problems. Even though, a classical weighted-sum approach can be used to get a few points on the Pareto-optimal front, finding the transition point accidentally with a particular weight vector will be highly unlikely.

## 4.2 Higher-Level Innovizations

Before we leave this case study, we would like to raise another important aspect of the innovization procedure. Since an analysis is performed on the solutions obtained by solving a particular optimization problem (that is, for fixed values of all problem parameters), one may wonder how the innovized results will change if different parameter values were used. In the context of the above truss-structure design, the parameters kept fixed for the entire analysis were: (i) upper limit of developed stress,  $S_{\max}$ , (ii) upper limit of cross-sectional areas,  $A_{\max}$ , (iii) lower and upper bound of  $y$ . It would be interesting to investigate whether the innovized principles deciphered above will still be valid parametrically for variations of these parameters! For example, one may think that the reason for the fixed- $x_2$  solutions (near smallest stress value) occurred due to the use of a small  $A_{\max}$ . It may be worthwhile to ponder whether the two-pronged behavior of the Pareto-optimal front observed above would still remain, if the cross-sectional limit  $A_{\max}$  is increased.

To get a complete idea of the innovized principles, one needs to redo the multi-objective optimization runs for different values of problem parameters and perform further analysis. Figure 7 shows the Pareto-optimal fronts obtained with different  $A_{\max}$  values and by keeping rest all parameters the same as before. Interestingly, in all simulations the two-pronged behavior

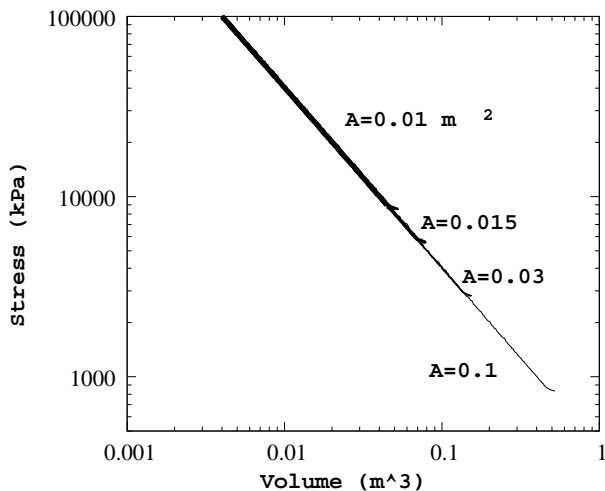


Figure 7: Pareto-optimal fronts for different values of  $A_{\max}$  show two-pronged behavior for the truss-structure design problem.

appear, meaning that the property of fixed- $y$  solutions for smaller volume solutions followed by fixed- $x_2$  solutions for smaller stress values is universal. A higher-level innovizations for the above truss-structure design problems are as follows:

1. As long as the required cross-sectional areas can be accepted, there exists an optimum  $y$ . By fixing  $y$  at this optimal value, a trade-off between stress and volume can be obtained by directly changing  $x_1$  and  $x_2$  by an identical rate.
2. Since  $x_2$  (in this configuration) would reach the upper limit faster than  $x_1$  due to its requirement of carrying a larger load, for any further reduction in stress value,  $x_2$  must be kept fixed at the upper bound and  $y$  should be increased till allowed. While doing so, the optimal procedure would be to reduce  $x_1$ . Thus, the minimum-stress configuration would be for the maximum value of  $x_2$  and for the largest value of  $y$  or the smallest value of  $x_1$ , whichever happens faster.
3. Figure 7 also shows that all fronts produce the same relationship  $SV \approx 400$  kN for optimality. Since,  $y = 2$  is an optimal solution for any  $A_{\max}$ , ideally,  $SV = 2 \times 20(16 + y^2)/y$  or 400 kN for all cases. Thus, for all optimal trusses having no bounds on cross-sectional size, an optimal truss will have  $SV = 400$  kN.

Similarly, further higher-level innovizations can be investigated by varying other fixed parameters and more insights can be revealed.

Two aspects are clear from the above discussion. The evolutionary multi-objective optimizer (NSGA-II) is capable of finding solutions close to the Pareto-optimal front and an analysis of the obtained solutions can reveal important information about the problem which may be difficult to achieve by an exact mathematical analysis. We now consider more difficult problems.

## 5 Gear Train Design

A compound gear train is to be designed to achieve a specific gear ratio between the driver and driven shafts (Figure 8). The problem considered here is a modification to the problem solved

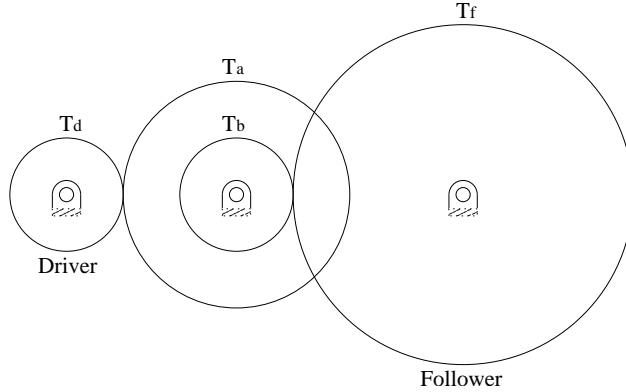


Figure 8: A gear train.

elsewhere [14, 4]. The objective of this gear train design is to find the number of teeth in each of the four gears so as to (i) minimize the error between the obtained gear ratio and a required gear ratio of 6.931:1 and (ii) minimize the maximum size of four gears. Since gear diameter is proportional to number of teeth which must be an integer, both objectives can be written in terms of four integer decision variables:  $\mathbf{x} = (x_1, x_2, x_3, x_4) = (T_d, T_b, T_a, T_f)$ . We write the two-objective optimization problem as follows:

$$\begin{aligned}
 &\text{Minimize} && f_1(\vec{x}) = \left| 6.931 - \frac{x_3 x_4}{x_1 x_2} \right|, \\
 &\text{Minimize} && f_2(\vec{x}) = \max(x_1, x_2, x_3, x_4), \\
 &\text{Subject to} && \frac{f_1(\vec{x})}{6.931} \leq 0.5, \\
 &&& 12 \leq x_1, x_2, x_3, x_4 \leq 60, \\
 &&& \text{all } x_i\text{'s are integers.}
 \end{aligned} \tag{8}$$

The constraint ensures that the error between obtained gear ratio and the desired gear ratio is not more than the 50% of the desired gear ratio. The decision variables are treated as integers and handled using six-bit binary strings in NSGA-II and single-point crossover and bit-wise mutation operators [11] are used. The all-zero string is coded to represent  $T_i = 12$  (for  $i = 1, \dots, 4$ ) and all-one string is coded to represent  $T_i = 75$ . A constraint  $T_i \leq 60$  is then used to make sure that the number of gear teeth in the range [12,60] are emphasized.

The individual minimum solutions obtained using single-objective GAs and NSGA-II are shown in Table 2. The Pareto-optimal front obtained using NSGA-II is shown in Figure 9. Due to

Table 2: The extreme solutions for the gear train design problem.

Solution	$x_1$	$x_2$	$x_3$	$x_4$	$f_1$	$f_2$
Min. Error	20	13	53	34	$2.3077(10^{-4})$	53
Min. of max. size of any gear	12	12	22	23	3.4171	23

the discreteness of the decision space, the non-dominated solutions are clustered to a few solutions in the objective space. These optimized solutions are then verified using the normal-constraint method (NCM). The obtained NCM solutions are also plotted in Figure 9.

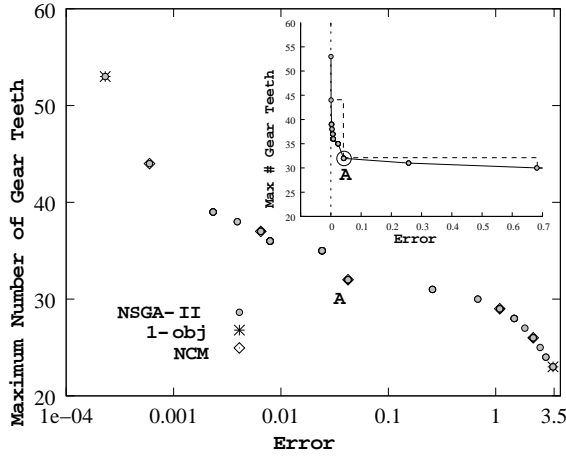


Figure 9: NSGA-II solutions show a trade-off between two objectives for the gear-train design problem. Single-objective and NCM solutions are also shown.

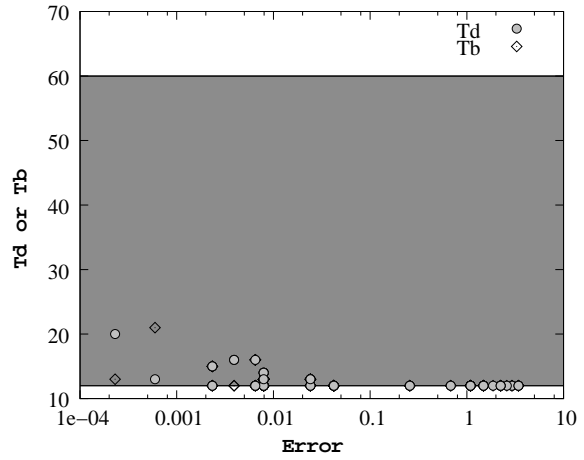


Figure 10: Gears  $d$  and  $b$  are assigned small number of teeth in the gear-train design problem.

### 5.1 Innovized Principles

Next, we analyze the NSGA-II solutions to decipher any commonality principles:

1. To minimize the second (size) objective, gears  $d$  and  $b$  have almost the smallest allowable number of teeth, as shown in Figure 10. The allowable limits on the gear-teeth (12 to 60) are shown shaded. In order to achieve a small normalized error (less than 0.1) in the overall gear-ratio from the desired value (6.931), in these gear-trains  $T_b$  and  $T_d$  values are required to be adjusted somewhat, but they still remain close to their respective lower bounds.
2. The maximum size of four gears occurs either for gear  $a$  or for gear  $f$ , a matter although intuitive, comes out as an outcome.
3. To reveal an interesting matter, Figure 11 plots the first-stage ratio ( $T_a/T_d$ ) with the second-stage ratio ( $T_f/T_b$ ) for all optimized solutions. It is clear that there are two types of solutions:

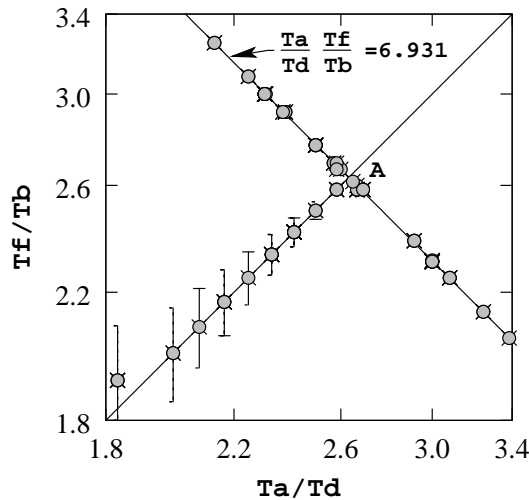


Figure 11: Two types of gear-trains are discovered as optimal.

- (i) gear-trains which have very small error (say, less than 0.1), that is, the product of the second and first-stage ratios is almost equal to the desired overall ratio (6.931:1) and (ii) gear-trains which have comparatively larger error from the desired gear ratio. Interestingly, for these latter gear-trains (a vertical error-bar on them indicates the error), both the first and the second-stage ratios are identical (except the one with the largest error). Although a large error can happen for many different combinations of errors in two stages, the minimization of the second objective (maximum number of gear teeth) causes both stages of gear-ratios to be identical – a matter which is not quite intuitive, but comes out as an innovized principle to this problem.
4. However, when the error is small (say, less than 0.1), although a gear-train (solution A (12, 12, 32, 31) in the inset plot of Figure 9) with almost identical gear ratios (first stage  $32/12 = 2.667$  and second-stage  $31/12 = 2.583$ ) (ideally,  $\sqrt{6.931} = 2.633$ ) exists in the Pareto-optimal set, there are certainly many other ways (making the product  $\frac{T_a}{T_d} \frac{T_f}{T_b}$  almost equal to 6.931) to achieve the overall gear ratio, as shown in Figure 11. It is also interesting to note that solution A in Figure 9 is a *knee* solution. In order to move to neighboring solutions in either objective, a comparatively larger sacrifice in one objective must be made to have a small gain in the other objective. From a consideration of both objectives, this solution would be an ideal choice to a decision-maker and an investigation of the obtained solutions also reveals that this solution makes an almost equal distribution of gear-ratios between two stages and also produces a small error in overall gear-ratio from the desired value.
  5. In the category of small-error gear-trains, exactly half of them have larger first-stage ratio than that in the second stage and other half have larger second-stage ratio than that in the first stage. This is apparent as the combined gear-ratio of  $(T_a/T_d) \cdot (T_f/T_b) = 6.931$  can be achieved for  $T_a/T_d = \alpha$  and  $T_f/T_b = \beta$  making  $\alpha \cdot \beta = 6.931$ . An identical combined gear ratio can also be achieved by swapping the first-stage gears with the second-stage gears, thereby making  $T_a/T_d = \beta$  and  $T_f/T_b = \alpha$ .

This example, though simple again, brings out a number of interesting properties of a gear-train design problem. Importantly, this study also depicts that NSGA-II and other procedures described here are also capable to be applied to non-linear integer programming problems.

## 6 Multiple-Disk Clutch Brake Design

In this problem, a multiple clutch brake [20], as shown in Figure 12, needs to be designed. Two conflicting objectives are considered: (i) minimization of mass ( $f_1$  in kg) of the brake system and (ii) minimization of stopping time ( $T$  in s). There are five decision variables:  $\vec{x} = (r_i, r_o, t, F, Z)$ , where  $r_i$  is the inner radius in mm,  $r_o$  is the outer radius in mm,  $t$  is the thickness of discs in mm,  $F$  is the actuating force in N and  $Z$  is the number of friction surfaces (or discs). All five variables are considered discrete and their allowable values are given below:

$$\begin{aligned}
 r_i &= (60, 61, 62, \dots, 78, 79, 80)\text{mm}, \\
 r_o &= (90, 91, 92, \dots, 108, 109, 110)\text{mm}, \\
 t &= (1, 1.5, 2, 2.5, 3)\text{mm}, \\
 F &= (600, 610, 620, \dots, 980, 990, 1000)\text{N}, \\
 Z &= (2, 3, 4, 5, 6, 7, 8, 10).
 \end{aligned}$$

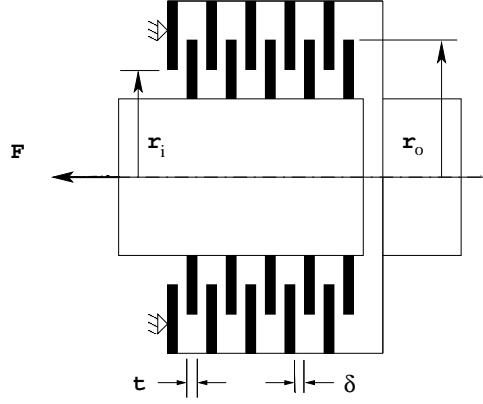


Figure 12: A multiple-disk clutch brake.

The optimization problem is formulated below:

$$\begin{aligned}
& \text{Minimize } f_1(\vec{x}) = \pi(x_2^2 - x_1^2)x_3(x_5 + 1)\rho, \\
& \text{Minimize } f_2(\vec{x}) = T = \frac{I_z\omega}{M_h + M_f}, \\
& \text{Subject to } g_1(\vec{x}) = x_2 - x_1 - \Delta R \geq 0, \\
& g_2(\vec{x}) = L_{\max} - (x_5 + 1)(x_3 + \delta) \geq 0, \\
& g_3(\vec{x}) = p_{\max} - p_{rz} \geq 0, \\
& g_4(\vec{x}) = p_{\max}V_{sr,\max} - p_{rz}V_{sr} \geq 0, \\
& g_5(\vec{x}) = V_{sr,\max} - V_{sr} \geq 0, \\
& g_6(\vec{x}) = M_h - sM_s \geq 0, \\
& g_7(\vec{x}) = T \geq 0, \\
& g_8(\vec{x}) = T_{\max} - T \geq 0, \\
& r_{i,\min} \leq x_1 \leq r_{i,\max}, \\
& r_{o,\min} \leq x_2 \leq r_{o,\max}, \\
& t_{\min} \leq x_3 \leq t_{\max}, \\
& 0 \leq x_4 \leq F_{\max}, \\
& 2 \leq x_5 \leq Z_{\max}.
\end{aligned} \tag{9}$$

The parameters are given below:

$$\begin{aligned}
M_h &= \frac{2}{3}\mu x_4 x_5 \frac{x_2^3 - x_1^3}{x_2^2 - x_1^2} \text{ N}\cdot\text{mm}, & \omega &= \pi n / 30 \text{ rad/s}, & A &= \pi(x_2^2 - x_1^2) \text{ mm}^2, & p_{rz} &= \frac{x_4}{A} \text{ N/mm}^2, \\
V_{sr} &= \frac{\pi R_{sr} n}{30} \text{ mm/s}, & R_{sr} &= \frac{2}{3} \frac{x_2^3 - x_1^3}{x_2^2 - x_1^2} \text{ mm}, & \Delta R &= 20 \text{ mm}, & L_{\max} &= 30 \text{ mm}, \\
\mu &= 0.5, & p_{\max} &= 1 \text{ MPa}, & \rho &= 0.0000078 \text{ kg/mm}^3, & V_{sr,\max} &= 10 \text{ m/s}, \\
s &= 1.5, & T_{\max} &= 15 \text{ s}, & n &= 250 \text{ rpm}, & M_s &= 40 \text{ Nm}, \\
M_f &= 3 \text{ Nm}, & I_z &= 55 \text{ kg}\cdot\text{m}^2, & \delta &= 0.5 \text{ mm}, & r_{i,\min} &= 60 \text{ mm}, \\
r_{i,\max} &= 80 \text{ mm}, & r_{o,\min} &= 90 \text{ mm}, & r_{o,\min} &= 110 \text{ mm}, & t_{\min} &= 1.5 \text{ mm}, \\
t_{\max} &= 3 \text{ mm}, & F_{\max} &= 1,000 \text{ N}, & Z_{\max} &= 9.
\end{aligned}$$

Individual minimum solutions are found by a single-objective NSGA-II and are shown in Table 3. The trade-off between two objectives is clear from the table. The Pareto-optimal front obtained using NSGA-II is shown in Figure 13. The extreme solutions shown in the table are also members of the Pareto-optimal front. The front is also verified by finding a number of optimal solutions using the NC method. The two extreme solutions shown in Table 3 are also identical to those reported elsewhere [20].

## 6.1 Innovized Principles

Following observations are made by analyzing the NSGA-II results.

Table 3: The extreme solutions for the multiple-disk clutch brake design.

Solution	$x_1$ (mm)	$x_2$ (mm)	$x_3$ (mm)	$x_4$ (N)	$x_5$	$f_1$ (kg)	$f_2$ (s)
Min. brake mass	70	90	1.5	1000	3	0.4704	11.7617
Min. stopping time	80	110	1.5	1000	9	2.0948	3.3505

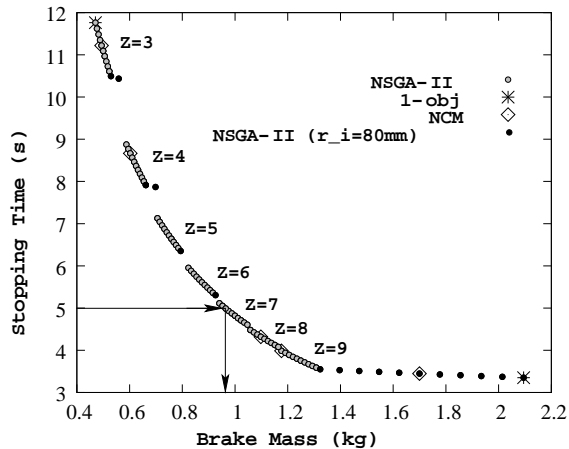


Figure 13: NSGA-II solutions for the clutch brake design problem.

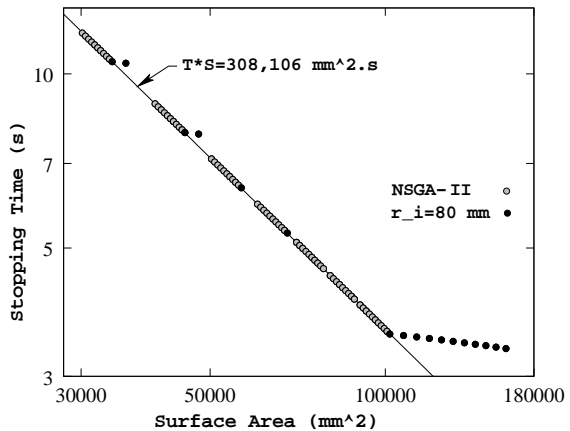


Figure 14: Stopping time (s) versus braking area ( $\text{mm}^2$ ) for the optimal solutions of the clutch brake design problem.

1. The Pareto-optimal front is fragmented into a number of contiguous regions of identical  $Z$  values, as shown in Figure 13. This means that fixing the number of discs is the highest-level decision-making process by which the location of specific stopping time and brake mass value get more or less set. This is not an intuitive matter, as the solutions on the Pareto-optimal front could have been ordered in any arbitrary manner. But for solutions to be optimal, the range of brakes from the least-weight design to quickest-acting design must be achieved with a monotonically increasing number of discs. For the smaller-weight solutions, fewer number of discs are needed, whereas for a quicker-acting design, the number of discs required are more. A design with only two discs ( $Z = 2$ ) becomes infeasible with respect to the maximum stopping time constraint ( $g_8(\vec{x})$ ) chosen in this study and hence does not appear on the optimal frontier. Since  $Z_{\max} = 9$  is chosen,  $Z = 10$  solutions also do not appear as optimal.
2. Interestingly, there are two distinct relationships observed among the solutions of the Pareto-optimal front. For every fixed- $Z$  portion of the front, there is a trade-off which starts with a small value of brake-mass having smallest values of  $r_i$  (70 mm) and  $r_o$  (90 mm), but in order to remain optimal both radii increase linearly by maintaining a difference of exactly  $\Delta R = 20$  mm, making the constraint  $g_1$  active. When  $r_i$  reaches its maximum limit (80 mm),  $r_i$  remains constant at this upper limit, but  $r_o$  keeps on increasing to produce faster stopping time solutions. These fixed- $r_i$  solutions are marked in filled circles in Figure 13. For example, with  $Z = 3$ , there are two such solutions which are Pareto-optimal.
3. Interestingly, for all optimal solutions, the following decision variables take identical values:

$$t = 1.5\text{mm}, \quad F = 1,000\text{N}.$$

The disc thicknesses ( $t$ ) of all solutions are identical to the lower allowable value ( $t_{\min} = 1.5$  mm) and the applied force must be set to the largest allowable value ( $F_{\max} = 1,000$  N).

These innovative relationships for an optimal solution is far from being intuitive and can only be inferred from the obtained optimized data.

4. It is also interesting to note that the stopping time ( $T$ ) is inversely proportional to the total braking area ( $S$ ) of the system, as shown in Figure 14. Although it may be intuitive to a designer that a quicker stopping time solution is expected to be achieved for a braking system having a larger braking area, NSGA-II solutions bring out an exact relationship ( $T \cdot S = 308,106 \text{ mm}^2 \cdot \text{s}$ ) between the two quantities in this problem. Since the thickness of the discs is found to be exactly the same for all optimal solutions, the mass (first objective) and braking surface area are proportional to each other. Figure 13 also shows an inverse relationship between the two objectives. It is also interesting to note that for solutions having the inner disc radius more than its allowed upper limit (80 mm), as shown in the Figure 14 with filled circles, the above inverse relationship does not hold.

As indicated above, it is clear from the results that fixing the number of discs is the highest-level decision-making in this design process. Say for example, if we need to design a brake system capable of stopping in a maximum of 5 seconds, Figure 13 immediately indicates that a minimum of  $Z = 7$  discs are needed with a smallest weight of 0.964 kg, requiring  $r_i = 72 \text{ mm}$  and  $r_o = 92 \text{ mm}$ . Any optimal design with a particular stopping time  $T$  must have an overall surface area of contact equal to  $S = 308,106/T \text{ mm}^2$ . Moreover, if a brake with a stopping time in the range 4.6 seconds to about 5.1 seconds is required, the optimal design should have seven discs with its weight ranging between 0.941 kg to 1.047 kg. Thus, Figure 13 and the corresponding decision variables values can be used as a ‘recipe’ of arriving at an optimal design for a particular desired performance of the braking system. Moreover, the use of the smallest possible thickness of discs and largest possible applied load would ensure working of the brake system at its optimal performance.

## 6.2 Higher-Level Innovations

It seems from the above simulation runs that the parameter  $r_{i,\max}$  is an important one. In order to investigate the effect of this parameter on the obtained Pareto-optimal solutions, we rerun NSGA-II for two other  $r_{i,\max}$  values (85 and 90 mm) and plot the frontiers in Figure 15. In both these cases,  $\Delta R = 20 \text{ mm}$ ,  $t = 1.5 \text{ mm}$ ,  $F = 1,000 \text{ N}$  remain as innovizations. Three higher-level

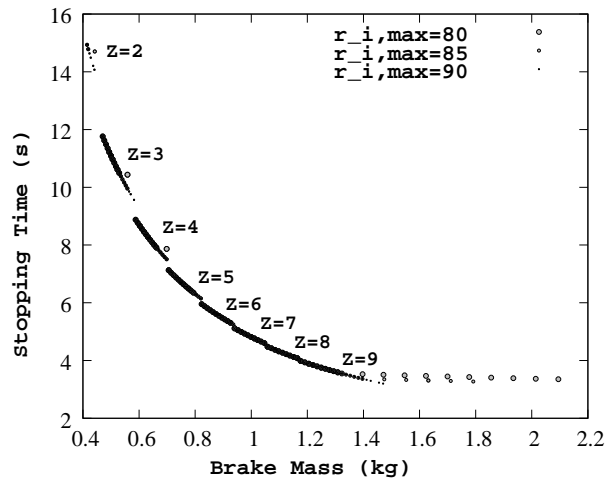


Figure 15: Effect of  $r_{i,\max}$  on the trade-off solutions of the clutch brake design problem.

innovized principles are obtained from this study:

1. With larger upper limit of  $r_i$ , the gap between trade-off fragments of two consecutive  $Z$  values reduce. Thus, the deviation of optimal solutions (shown with filled circles) from fixed  $T \cdot S$  relationship observed in Figure 14 is purely due to the fixation of the upper limit of  $r_i$ .
2. Solutions obtained with fixed  $r_i = r_{i,\max}$  are better for a larger  $r_{i,\max}$  value. However, solutions having  $r_i < r_{i,\max}$  and obtained with different  $r_{i,\max}$  values all follow the  $T \cdot S = 308,106$  relationship. Thus, the  $T$ - $S$  relationship is independent of the choice of  $r_{i,\max}$ .
3. With larger upper limit of  $r_i$ , more light-weight brakes with only  $Z = 2$  discs having a stopping time less than or equal to 15 seconds are possible. Recall that with  $r_{i,\max} = 80$  mm,  $Z = 2$  solutions were infeasible. These light-weight brakes have larger  $r_i$  and  $r_o$  values than the earlier case, thereby allowing to have a larger surface area per disc.

With the limit of  $r_{i,\max} = 85$  or  $90$  mm, the lightest weight brake weighs  $0.4145$  kg having  $r_i = 84$  mm and  $r_o = 104$  mm, as opposed to  $0.4704$  kg obtained with  $r_{i,\max} = 80$  mm. Similarly, a quicker-acting brake can be designed with an increase in  $r_{i,\max}$  ( $T = 3.20$  seconds with  $r_{i,\max} = 90$  mm compared to  $T = 3.35$  seconds with  $r_{i,\max} = 80$  mm).

## 7 Spring Design

A helical compression spring needs to be designed for minimum volume and for minimum developed stress. Three variables are used for this purpose: the wire diameter  $d$  which is a discrete variable taking a few values mentioned below, the mean coil diameter  $D$  which is a real-valued parameter varied in the range  $[1,30]$  in, and the number of turns  $N$ , which is an integer value varied in the range  $[1,32]$ . The wire diameter  $d$  takes one of 42 non-equi-spaced values (as given in [14]). Denoting the variable vector  $\vec{x} = (x_1, x_2, x_3) = (N, d, D)$ , we write the two-objective, eight-constraint optimization problem as follows:

$$\begin{aligned}
&\text{Minimize} && f_1(\vec{x}) = 0.25\pi^2 x_2^2 x_3 (x_1 + 2), \\
&\text{Minimize} && f_2(\vec{x}) = \frac{8KP_{max}x_3}{\pi x_2^3}, \\
&\text{Subject to} && g_1(\vec{x}) = l_{max} - \frac{P_{max}}{k} - 1.05(x_1 + 2)x_2 \geq 0, \\
&&& g_2(\vec{x}) = x_2 - d_{min} \geq 0, \\
&&& g_3(\vec{x}) = D_{max} - (x_2 + x_3) \geq 0, \\
&&& g_4(\vec{x}) = C - 3 \geq 0, \\
&&& g_5(\vec{x}) = \delta_{pm} - \delta_p \geq 0, \\
&&& g_6(\vec{x}) = \frac{P_{max} - P}{k} - \delta_w \geq 0, \\
&&& g_7(\vec{x}) = S - \frac{8KP_{max}x_3}{\pi x_2^3} \geq 0, \\
&&& g_8(\vec{x}) = V_{max} - 0.25\pi^2 x_2^2 x_3 (x_1 + 2) \geq 0, \\
&&& x_1 \text{ is integer, } x_2 \text{ is discrete, } x_3 \text{ is continuous.}
\end{aligned} \tag{10}$$

The parameters used are as follows:

$$\begin{aligned}
K &= \frac{4C-1}{4C-4} + \frac{0.615x_2}{x_3}, & P &= 300 \text{ lb}, & D_{max} &= 3 \text{ in}, & k &= \frac{Gx_2^4}{8x_1x_3^3}, \\
P_{max} &= 1,000 \text{ lb}, & \delta_w &= 1.25 \text{ in}, & \delta_p &= \frac{P}{k}, & l_{max} &= 14 \text{ in}, \\
\delta_{pm} &= 6 \text{ in}, & S &= 189 \text{ ksi}, & d_{min} &= 0.2 \text{ in}, & C &= x_3/x_2, \\
G &= 11,500,000 \text{ lb/in}^2, & V_{max} &= 30 \text{ in}^3.
\end{aligned}$$

The 42 discrete values of  $d$  are given below:

$$\mathbf{d} = \begin{pmatrix} 0.009, & 0.0095, & 0.0104, & 0.0118, & 0.0128, & 0.0132, \\ 0.014, & 0.015, & 0.0162, & 0.0173, & 0.018, & 0.020, \\ 0.023, & 0.025, & 0.028, & 0.032, & 0.035, & 0.041, \\ 0.047, & 0.054, & 0.063, & 0.072, & 0.080, & 0.092, \\ 0.105, & 0.120, & 0.135, & 0.148, & 0.162, & 0.177, \\ 0.192, & 0.207, & 0.225, & 0.244, & 0.263, & 0.283, \\ 0.307, & 0.331, & 0.362, & 0.394, & 0.4375, & 0.5. \end{pmatrix}$$

The design variables  $d$  and  $D$  are treated as real-valued parameters in the NSGA-II with  $d$  taking discrete values from the above set and  $N$  is treated with a five-bit binary string, thereby coding integers in the range [1,32]. While SBX and polynomial mutation operators are used to handle  $d$  and  $D$ , a single-point crossover and bit-wise mutation are used to handle  $N$ .

First, to obtain the individual minimum solutions, we use NSGA-II for solving each objective alone and obtain the solutions shown in Table 4. The non-dominated front found by NSGA-II

Table 4: The extreme solutions for the spring design problem.

Solution	$x_1$ (in)	$x_2$ (in)	$x_3$	$f_1$ (in <sup>3</sup> )	$f_2$ (psi)
Min. Volume	9	0.283	1.223	2.659	187,997.203
Min. Stress	21	0.5	1.969	27.943	56,626.148

also contains the same extreme solutions. Figure 16 shows the non-dominated front obtained by NSGA-II. The solutions obtained by several starting solutions by the NC method are also shown

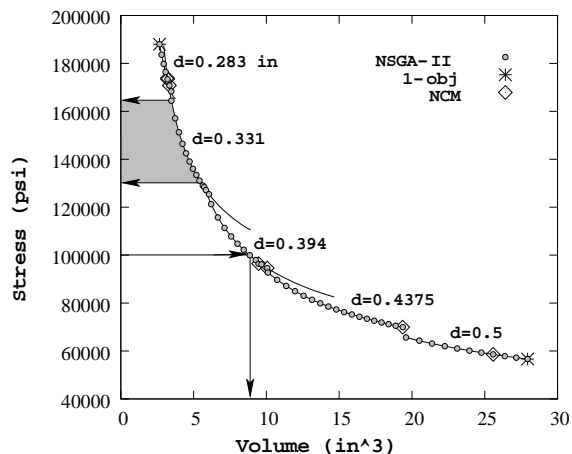


Figure 16: Pareto-optimal front obtained using NSGA-II for the spring design problem.

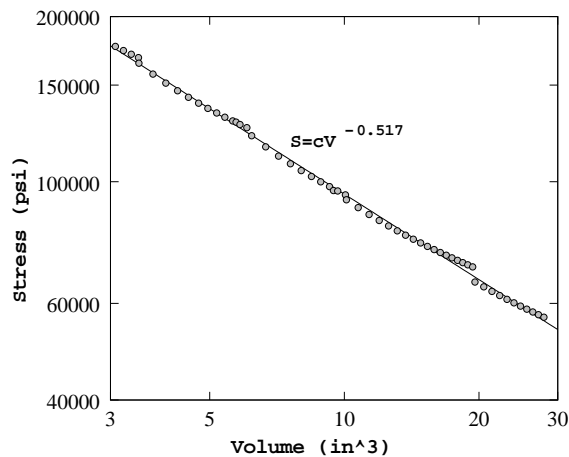


Figure 17: Optimal solutions follow a relationship between volume (size) and stress (performance) in the spring design problem.

in the figure. A good agreement between single-objective results, NSGA-II results and NCM results give us confidence in the optimality of the obtained front. For this problem, only the minimum-volume solution obtained using a differential evolution based approach was reported elsewhere [16] and it matches with the obtained NSGA-II solution.

## 7.1 Innovized Principles

Let us now analyze the optimal solutions to find if there are any innovized principles which can be gathered about the spring design problem. We observe the following principles:

1. The Pareto-optimal front is fragmented and every fragment corresponds to a fixed value of wire diameter  $d$ , as shown in Figure 16. Of 42 different allowed  $d$  values, only five values make their places on the Pareto-optimal frontier. Here, fixing the  $d$  value fixes the range of optimal objective values on the Pareto-optimal frontier, thereby making the selection of this parameter the most important decision-making task in the design process.
2. Moreover, not every combination of  $D$  and  $N$  turns out to be optimal for these five values of  $d$ . Figure 16 also shows (with a solid line) the complete non-dominated front obtained by keeping  $d$  constant and using only  $D$  and  $N$  as decision variables. As evident from the figure, some part of each front does not qualify (gets dominated by members of other fragments) to remain as Pareto-optimal when all  $d$  values are allowed.
3. For an optimal solution having a small volume, a small  $d$  must be chosen. However, the smallest available wire diameter ( $d = 0.009$  in) is not an optimal choice. In fact, the smallest optimal wire diameter is  $d = 0.283$  in.
4. When the non-dominated solutions are plotted in a logarithmic scale (Figure 17), optimal objective values (volume ( $V$ ) and stress ( $S$ )) are found to have an interesting relationship:  $SV^{0.517} = \text{constant}$ .
5. An investigation of optimal values of  $N$  and  $D$  reveals that they vary as  $N \propto 1/D^3$  (shown in Figure 18). Since different fixed- $d$  plots are all parallel to each other, the above relationship remains the same for all obtained solutions.

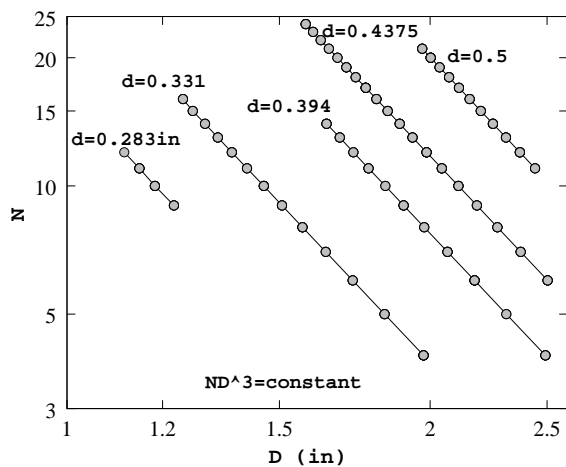


Figure 18: Optimal solutions follow  $ND^3 = \text{constant}$  relationship for the spring design problem.

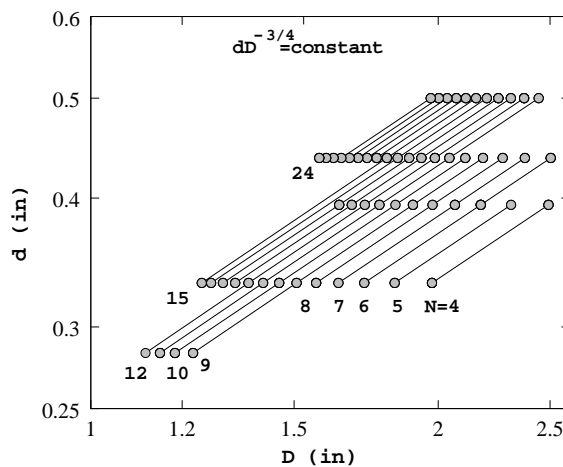


Figure 19: Optimal solutions follow  $dD^{-3/4} = \text{constant}$  relationship for the spring design problem.

6. Similarly, an analysis of optimal values of  $d$  and  $D$  reveals:  $d \propto D^{3/4}$  (shown in Figure 19) for all trade-off solutions.
7. Combining the two relationships, we conclude that  $ND^3/d^4$  is a constant for all non-dominated solutions. It is interesting to note that this quantity is proportional to the

inverse of spring constant  $k = Gd^4/(8ND^3)$ . By substituting the constant derived from the NSGA-II solutions, we obtain  $k = 560$  lb/in for all optimal solutions. This reveals an innovation for this spring design problem. In order to create an optimal solution, we simply need to have a spring with a fixed spring constant of 560 lb/in for the chosen parameters of the design problem. Obviously, one can have different combinations of  $d$ ,  $D$  and  $N$  to achieve this magical spring constant value. Figure 16 shows all such solutions which will make a non-dominated optimal combination of two objectives. To design an optimal spring having a small volume (or weight), the spring must be formed using a small sized wire, a small mandrel diameter and a few number of turns. Interestingly, a bigger-sized spring can also be designed with an identical spring constant by having a large sized wire, a large mandrel diameter and a large number of turns. The latter design, although has an identical spring constant to the former light-weight spring, will be able to withstand a larger amount of stress. What we have achieved with the proposed innovization procedure is a ‘recipe’ to arrive at different trade-off solutions (between size and strength), each having an identical spring constant of 560 lb/in, but having differing dimensions.

8. Another interesting aspect of the obtained NSGA-II solutions is that the constraint  $g_6$  is active for all solutions. By substituting the fixed parameters in the mathematical constraint function ( $g_6$ ), we obtain  $k = (1000 - 300)/1.25 = 560$  lb/in, thereby explaining the specific value of the spring constant observed in the obtained data above. Since no other constraints are active for all Pareto-optimal solutions, other constraints do not result in any other innovization.

The above innovized principles provide us with a *recipe* of designing a spring optimally. For example, if a spring has to be designed with a material having yield strength of 100,000 psi, Figure 16 clearly shows that an optimal design must be made from a wire of diameter  $d = 0.394$  in. Other design variables must take  $D = 1.779$  in and  $N = 11$  turns and the spring will have a volume of  $8.857$  in<sup>3</sup>. The results can also be interpreted as follows. If the designer is looking for designing a range of springs with materials having yield strength ranging from 130,000 psi to 165,000 psi, the optimal spring must be made from a wire of diameter 0.331 in, thereby requiring to maintain a small inventory for storing only one-sized wire for making optimal springs. What is also important here to note that all such springs will be *optimal* from a dual consideration of volume (size) and strength (performance). The information about specific wire diameters (only five out of chosen 42 different values) for optimality and a common property of having a fixed spring constant (of 560 lb/in) are all innovations, which will be difficult to arrive at, otherwise. In this particular problem, the chosen value of parameters  $G$ ,  $P_{\max}$ ,  $P$ , and  $\delta_w$  allowed these properties to emerge as innovations for a solution to be optimal. For some other parameter setting, some other innovized principles may have been evolved. But to find such important principles of design, our proposed methodology can be applied again (discussed in the next subsection) and it is not clear how else such vital and useful information about a problem can be learned by any other technique.

## 7.2 Higher-Level Innovizations

Next, we increase  $\delta_w$  to twice to its previous value, that is, we set  $\delta_w = 2.5$  in. When we redo the proposed innovization procedure, we once again observe that the constraint  $g_6$  is active for all solutions. Substituting other parameters, we then obtain  $k = (1000 - 300)/2.5 = 280$  lb/in, half of what was achieved previously. Substituting the new values of the design variables in the stiffness term  $k$ , we observe that all solutions possess more or less an identical  $k = 280$  lb/in, as can also be seen from Figure 20. We repeat the study for  $\delta_w = 0.625$  in and observe that the corresponding stiffness of solutions come close to  $k = 1,120$  lb/in. This clearly brings out an

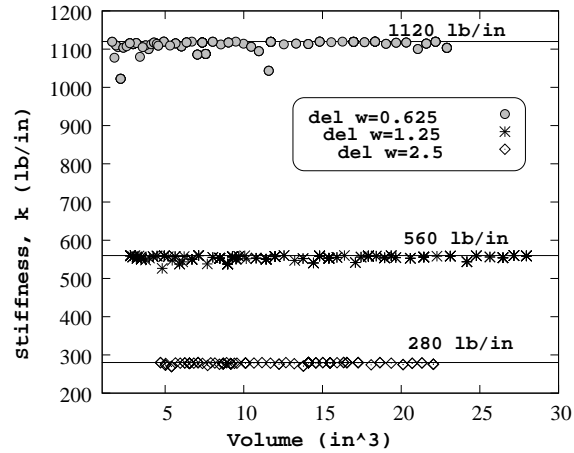


Figure 20: Different  $\delta_w$  causes different Pareto-optimal frontiers, each causing an identical spring stiffness in all its solutions.

important innovation: All Pareto-optimal solutions must have an identical spring stiffness and the stiffness value depends on the chosen values of fixed parameters.

## 8 Welded Beam Design

The welded beam design problem is well studied in the context of single-objective optimization [21]. A beam needs to be welded on another beam and must carry a certain load  $F$  (Figure 21). It is

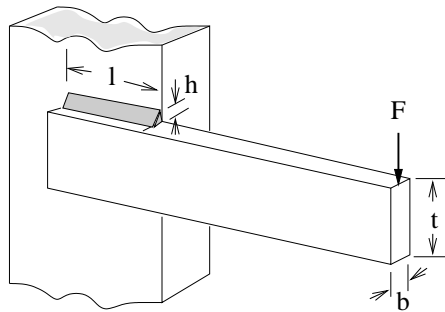


Figure 21: The welded beam design problem.

desired to find four design parameters (thickness of the beam,  $b$ , width of the beam  $t$ , length of weld  $\ell$ , and weld thickness  $h$ ) for which the cost of the beam is minimum and simultaneously the vertical deflection at the end of the beam is minimum. The overhang portion of the beam has a length of 14 in and  $F = 6,000$  lb force is applied at the end of the beam. It is intuitive that a design which is optimal from the cost consideration is not optimal from rigidity consideration (or end-deflection) and vice versa. Such conflicting objectives lead to interesting Pareto-optimal solutions. In the following, we present the mathematical formulation of the two-objective optimization problem of

minimizing cost and the end deflection [10, 5]:

$$\begin{aligned}
& \text{Minimize } f_1(\vec{x}) = 1.10471h^2\ell + 0.04811tb(14.0 + \ell), \\
& \text{Minimize } f_2(\vec{x}) = \frac{2.1952}{t^3b}, \\
& \text{Subject to } g_1(\vec{x}) \equiv 13,600 - \tau(\vec{x}) \geq 0, \\
& \quad g_2(\vec{x}) \equiv 30,000 - \sigma(\vec{x}) \geq 0, \\
& \quad g_3(\vec{x}) \equiv b - h \geq 0, \\
& \quad g_4(\vec{x}) \equiv P_c(\vec{x}) - 6,000 \geq 0, \\
& \quad 0.125 \leq h, b \leq 5.0, \\
& \quad 0.1 \leq \ell, t \leq 10.0.
\end{aligned} \tag{11}$$

There are four constraints. The first constraint makes sure that the shear stress developed at the support location of the beam is smaller than the allowable shear strength of the material (13,600 psi). The second constraint makes sure that normal stress developed at the support location of the beam is smaller than the allowable yield strength of the material (30,000 psi). The third constraint makes sure that thickness of the beam is not smaller than the weld thickness from a practical standpoint. The fourth constraint makes sure that the allowable buckling load (along  $t$  direction) of the beam is more than the applied load  $F$ . A violation of any of the above four constraints will make the design unacceptable. The stress and buckling terms are highly non-linear to design variables and are given as follows [21]:

$$\begin{aligned}
\tau(\vec{x}) &= \sqrt{(\tau')^2 + (\tau'')^2 + (\ell\tau'\tau'')/\sqrt{0.25(\ell^2 + (h+t)^2)}}, \\
\tau' &= \frac{6,000}{\sqrt{2}h\ell}, \\
\tau'' &= \frac{6,000(14 + 0.5\ell)\sqrt{0.25(\ell^2 + (h+t)^2)}}{2\{0.707h\ell(\ell^2/12 + 0.25(h+t)^2)\}}, \\
\sigma(\vec{x}) &= \frac{504,000}{t^2b}, \\
P_c(\vec{x}) &= 64,746.022(1 - 0.0282346t)tb^3.
\end{aligned}$$

Table 5 presents the two extreme solutions obtained by the single-objective GA and also by NSGA-II. An intermediate solution, T (which will be explained latter), obtained by NSGA-II, is also shown. Figure 22 shows these two extreme solutions and a set of Pareto-optimal solutions obtained using NSGA-II. The obtained front is verified by finding a number of Pareto-optimal

Table 5: The extreme solutions for the welded-beam design problem.

Solution	$x_1$ (h) (in)	$x_2$ ( $\ell$ ) (in)	$x_3$ (t) (in)	$x_4$ (b) (in)	$f_1$	$f_2$ (in)
Min. Cost	0.2443	6.2151	8.2986	0.2443	2.3815	0.0157
Min. Deflection	1.5574	0.5434	10.0000	5.0000	36.4403	4.3904( $10^{-4}$ )
Intermediate (T)	0.2326	5.3305	10.0000	0.2356	2.5094	0.0093

solutions using the NC method.

## 8.1 Innovized Principles

Let us now analyze the NSGA-II solutions to decipher innovized design principles:

1. Although Figure 22 shows an apparent inverse relationship between the two objectives, the logarithmic plot (inset) shows that there are two distinct behaviors between the objectives.

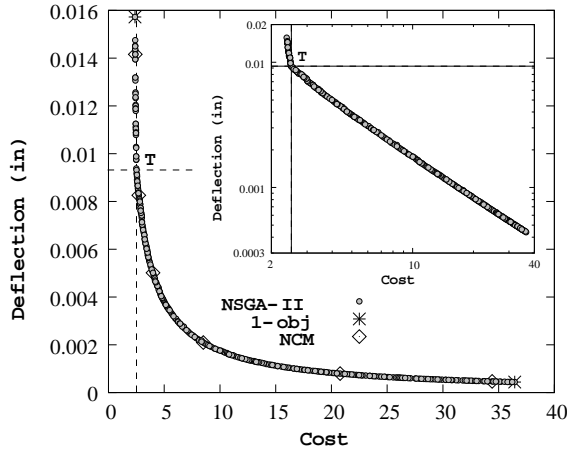


Figure 22: NSGA-II solutions are shown for the welded-beam design problem.

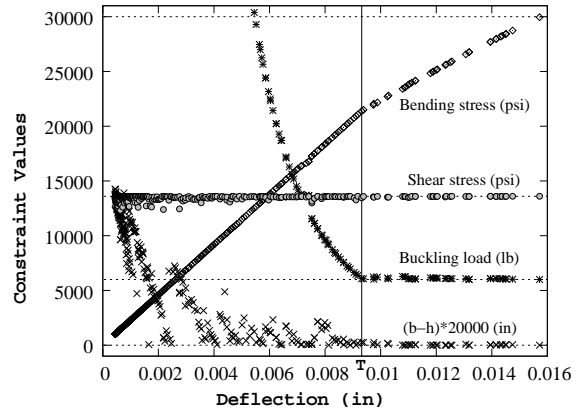


Figure 23: Constraint values of all Pareto-optimal solutions are shown for the welded-beam design problem.

From an intermediate transition solution T (shown in Table 5 and in Figure 22) near the smallest-cost (having comparatively larger deflection) solutions, objectives behave differently than in the rest of the trade-off region. For small-deflection solutions, the relationship is almost polynomial ( $f_1 \approx O(f_2^{-0.890})$ ).

2. Figure 23 plots the constraint values for all trade-off solutions. It is apparent that for all optimal solutions the shear stress constraint is most critical and active. For small-deflection (or large-cost) solutions, the chosen bending strength (30,000 psi) and allowable buckling load (6,000 lb) are quite large compared to the developed stress and applied load. Any Pareto-optimal solution must achieve the maximum allowable shear stress value (13,600 psi). Thus, in order to improve the design, selection of a material having a larger shear strength capacity would be wise.
3. The transition point (point T) between two trade-off behaviors (observed in Figure 22) happens mainly from the buckling consideration. Designs having larger deflection values (or smaller cost values) reduce the buckling load capacity, as shown in Figure 23. When the buckling load capacity becomes equal to the allowable limit (6,000 lb), no further reduction is allowed. This happens at a deflection value close to 0.00932 in (having a cost of 2.509).
4. Interestingly, there are further innovations with the design variables. For small-deflection solutions, the decision variable  $b$  must reduce inversely ( $b \propto 1/f_2$ ) with deflection objective ( $f_2$ ) to retain optimality. Since for these solutions, the shear stress constraint is only active and since the shear stress constraint does not involve the variable  $b$ , this variable does not get set by the constraint. On the other hand,  $b$  has an inverse effect between cost and deflection. Thus, the optimal solutions reflect a similar pattern of variation to  $b$ : a reduction in  $b$  causes a reduction in cost and an increase in deflection (Figure 23).
5. For small-deflection solutions, the decision variable  $t$  remains constant, as shown in Figure 24. This indicates that for most Pareto-optimal solutions, the height of the beam must be set to its upper limit. Although  $t$  causes an inverse effect to cost and deflection, as apparent from the equations, the active shear stress constraint involves  $t$ . Since shear stress value reduces with an increase in  $t$  (apparent from the formulation), it can be argued that fixing  $t$  to its upper limit would make a design optimal. Thus, if in practice solutions close

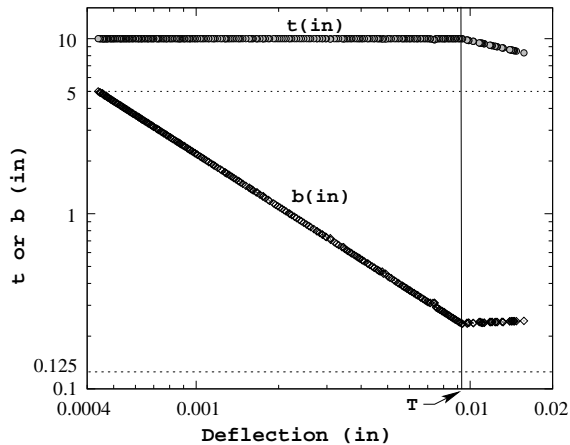


Figure 24: Variations of design variables  $t$  and  $b$  across the Pareto-optimal front are shown for the welded-beam design problem.

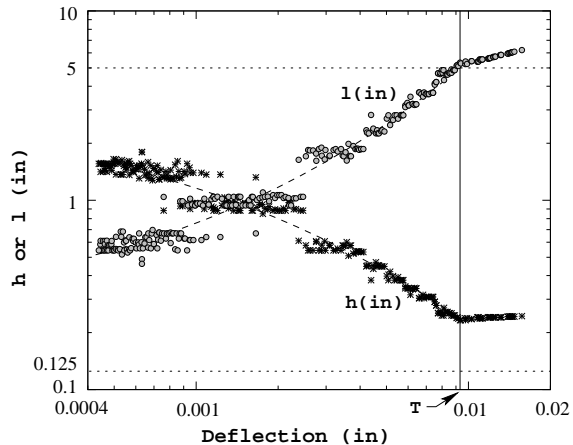


Figure 25: Variations of design variables  $h$  and  $\ell$  across the Pareto-optimal front are shown for the welded-beam design problem.

to the smallest-cost solution are not desired, a beam of identical height ( $t = 10$  in) may only be procured, thereby simplifying the inventory.

6. However, an increase of  $\ell$  and a decrease in  $h$  with an increase in deflection (or a decrease in cost) are not completely monotonic, as can be seen from Figure 25. These two phenomena are not at all intuitive and are also difficult to explain from the problem formulation. However, the innovized principles for arriving at optimal solutions seem to be as follows: for a reduced cost solution, keep  $t$  fixed to its upper limit, increase  $\ell$  and reduce  $h$  and  $b$ . This ‘recipe’ of design can be practiced only till the applied load is strictly smaller than the allowable buckling load.
7. Thereafter, any reduction in cost optimally must come from (i) reducing  $t$  from its upper limit, (ii) increasing  $b$ , and (iii) adjusting other two variables so as to make buckling, shear stress, and constraint  $g_4$  active. In these solutions, with decreasing cost, the dimensions are reduced in such a manner so as to make the bending stress to increase. Finally, the minimum cost solution occurs when the bending stress equals to the allowable strength (30,000 psi, as in Figure 23). At this solution all four constraints become active, so as to optimally utilize the materials for all four purposes.
8. To achieve very small cost solutions, the innovized principles are different: for a reduced cost solution, reduce  $t$  and increase  $\ell$ ,  $h$  and  $b$ . Thus, overall a larger  $\ell$  is needed to achieve a small cost solution.

## 8.2 Higher-Level Innovizations

Here, we redo the innovization procedure for one different value of three allowable limits: shear strength in constraint  $g_1$  is increased by 20%, bending strength in constraint  $g_2$  is increased by 20%, and buckling limit load in constraint  $g_4$  is reduced by 50%. We change them one at a time and keep the other parameters identical to their previous values. Figure 26 shows the corresponding Pareto-optimal frontiers for these three cases. Following innovizations are obtained:

1. It is clear that all three cases produce similar dual behavior (different characteristics on either side of a transition point) in the Pareto-optimal frontier, as was also observed in the

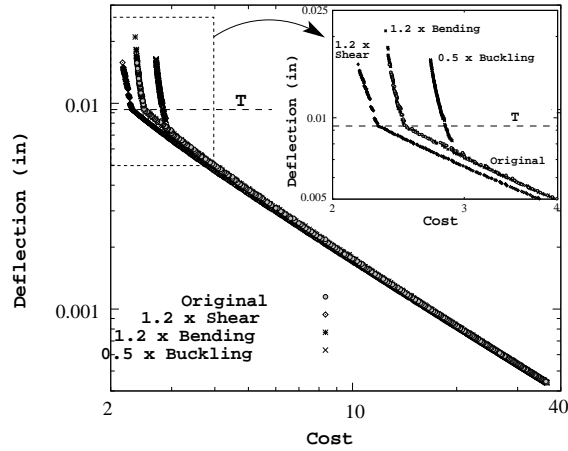


Figure 26: Effect of material strength and buckling load limit on the Pareto-optimal frontier for the welded-beam design problem.

previous case. All other innovations (such as  $t$  being constant and  $b$  being smaller with increasing deflection, etc.) mentioned earlier remains the same in all three cases.

2. The minimum-cost solution depends on all three constraint ( $g_1$ ,  $g_2$  and  $g_4$ ) limits, but the minimum-deflection solution only depends on the limit on shear stress constraint ( $g_1$ ). However, at this solution, variables  $t$  and  $b$  take their largest allowable values of 10 in and 5 in, respectively.
3. An increase of shear strength by 20% causes the solutions to change. Recall that the shear stress constraint ( $g_1$ ) was the most critical constraint in the original case. An increase in shear strength value also makes the constraint active for all new trade-off solutions. Since solutions change, a slightly different trade-off frontier emerges. Interestingly, the location of the transition point along deflection axis does not get changed (since the buckling load limit is not changed).
4. An increase of bending strength by 20% does not change smaller-deflection solutions. Since a higher bending limit is allowed now, better cost solutions are found. A solution with a cost of 2.3545 is now obtained with a deflection value of 0.021 in. The location of the transition point is unaffected by this change in bending strength value.
5. Finally, a decrease in the buckling load limit by 50% changes the location of the transition point (which moves towards a larger cost solution), however the rest of the original Pareto-optimal frontier remains identical to the original front.

Thus, we conclude with confidence that (i) shear strength has a major role to play in deciding the optimal variable combinations (the shear stress constraint remains active in all cases), (ii) bending strength has an effect on the smallest-cost solution alone, as only this solution makes the bending constraint active, and (iii) buckling load limit has the sole effect in locating the transition point on the Pareto-optimal front. These information provide adequate knowledge about relative importance of each constraint and variable interactions for optimally designing a welded-beam over an entire gamut of cost-deflection trade-off. It is unclear how such valuable innovative information could have been achieved otherwise merely from a mathematical problem formulation.

## 9 Conclusions

In this paper, we have introduced a new design procedure (through a new terminology, we called 'innovization procedure') based on multi-objective optimization and a post-optimality analysis of optimized solutions. We have argued that the task of a single-objective optimization results in a single optimum solution which may not provide enough information about useful relationships among design variables, constraints and objectives for achieving different trade-off solutions. On the other hand, consideration of at least two conflicting objectives of design should result in a number of optimal solutions, trading-off the two objectives. Thereafter, a post-optimality analysis of these optimal solutions should provide useful information and design principles about the problem, such as relationships among variables and objectives which are common among the optimal solutions and the differences which make the optimal solutions different from each other. We have argued that such information should often introduce new principles for optimal designs, thereby allowing designers to learn innovations about solving the problem at hand.

On a number of engineering design problems having mixed discrete and continuous design variables, many useful innovizations (innovative design principles) are deciphered. Interestingly, many such innovizations were not intuitive and not known before. The ease of application of the proposed innovization procedure has also become clear from different applications. It is also clear that the proposed procedure is useful and ready to be used in other more complex design tasks. The procedure will enable designers to perform the innovization task once and for all to the problem at hand and the knowledge thus gained will go a long way in understanding the intricacies of the problems and in solving such future design tasks. On another note, since the Pareto-optimal frontier obtained using NSGA-II are verified by other single-objective optimization techniques, the reported trade-off solutions also remain as 'benchmark' optimal solutions to these problems.

However, the innovization procedure suggested here must now be made more automatic and problem-independent as far as possible. In this regard, an efficient data-mining technique is in order to evolve innovative design relationships from the Pareto-optimal solutions. Although some apparent hurdles of this task have been pointed out in this paper, effort is underway at Kanpur Genetic Algorithms Laboratory (KanGAL) in this direction.

Finally, it is also worth mentioning that similar to the expectation of common properties to exist among Pareto-optimal solutions (as discovered and demonstrated amply in this paper), commonality principles may also be expected to exist in other kinds of trade-off solutions, such as among weakly Pareto-optimal solutions, locally Pareto-optimal solutions [6], and robust or reliable Pareto-optimal solutions [9]. It would be interesting then to investigate how the innovized relationships get changed from one type of optimal solutions to the other. For example, such an analysis may provide answers to questions such as how are *robust* Pareto-optimal solutions different from the Pareto-optimal solutions themselves! Another interesting extension of this study would be to consider three or more conflicting objectives of design and a resulting post-optimality analysis may yield higher-level innovizations than that may be obtained with the two-objective procedure. The ease and ability of NSGA-II to handle different vagaries of design variables (discrete, Boolean, real-valued etc.), nonlinearities in constraint and objective functions, scalability in problem size, and multi-modality and multi-objectivity in problem formulations allow such an innovization task tractable and worth performing.

## References

- [1] H. P. Benson. Existence of efficient solutions for vector maximization problems. *Journal of Optimization Theory and Applications*, 26(4):569–580, 1978.

- [2] V. Chankong and Y. Y. Haimes. *Multiobjective Decision Making Theory and Methodology*. New York: North-Holland, 1983.
- [3] C. A. C. Coello, D. A. VanVeldhuizen, and G. Lamont. *Evolutionary Algorithms for Solving Multi-Objective Problems*. Boston, MA: Kluwer Academic Publishers, 2002.
- [4] K. Deb. Mechanical component design using genetic algorithms. In D. Dasgupta and Z. Michalewicz, editors, *Evolutionary Algorithms in Engineering Applications*, pages 495–512. New York: Springer-Verlag, 1997.
- [5] K. Deb. An efficient constraint handling method for genetic algorithms. *Computer Methods in Applied Mechanics and Engineering*, 186(2–4):311–338, 2000.
- [6] K. Deb. *Multi-objective optimization using evolutionary algorithms*. Chichester, UK: Wiley, 2001.
- [7] K. Deb. Unveiling innovative design principles by means of multiple conflicting objectives. *Engineering Optimization*, 35(5):445–470, 2003.
- [8] K. Deb, S. Agrawal, A. Pratap, and T. Meyarivan. A fast and elitist multi-objective genetic algorithm: NSGA-II. *IEEE Transactions on Evolutionary Computation*, 6(2):182–197, 2002.
- [9] K. Deb and H. Gupta. Searching for robust Pareto-optimal solutions in multi-objective optimization. In *Proceedings of the Third Evolutionary Multi-Criteria Optimization (EMO-05) Conference (Also Lecture Notes on Computer Science 3410)*, pages 150–164, 2005.
- [10] K. Deb and A. Kumar. Real-coded genetic algorithms with simulated binary crossover: Studies on multi-modal and multi-objective problems. *Complex Systems*, 9(6):431–454, 1995.
- [11] D. E. Goldberg. *Genetic Algorithms for Search, Optimization, and Machine Learning*. Reading, MA: Addison-Wesley, 1989.
- [12] D. E. Goldberg. *The design of innovation: Lessons from and for Competent genetic algorithms*. Kluwer Academic Publishers, 2002.
- [13] J. Jahn. *Vector optimization*. Berlin, Germany: Springer-Verlag, 2004.
- [14] B. K. Kannan and S. N. Kramer. An augmented lagrange multiplier based method for mixed integer discrete continuous optimization and its applications to mechanical design. *ASME Journal of Mechanical Design*, 116(2):405–411, 1994.
- [15] P. Korhonen, S. Salo, and R. Steuer. A heuristic for estimating nadir criterion values in multiple objective linear programming. *Operations Research*, 45(5):751–757, 1997.
- [16] J. Lampinen and I. Zelinka. Mechanical engineering design optimization by differential evolution. In D. Corne, M. Dorigo, and F. Glover, editors, *New Ideas in Optimization*, pages 127–146. Berkshire, UK: McGraw-Hill, 1999.
- [17] Siemens Ltd. TEFC 3 phase squirrel cage induction motor catalogue, <http://globaludyog.com/pumps/sl.htm>.
- [18] A. Messac and C. A. Mattson. Normal constraint method with guarantee of even representation of complete pareto frontier. *AIAA Journal*, in press.
- [19] K. Miettinen. *Nonlinear Multiobjective Optimization*. Kluwer, Boston, 1999.

- [20] A. Osyczka. *Evolutionary algorithms for single and multicriteria design optimization*. Heidelberg: Physica-Verlag, 2002.
- [21] G. V. Reklaitis, A. Ravindran, and K. M. Ragsdell. *Engineering Optimization Methods and Applications*. New York : Wiley, 1983.